*Rapid Communication* J. Biochem. 120, 14-17 (1996)

# Three-Dimensional Structure of Porcine Kidney D-Amino Acid Oxidase at 3.0 Å Resolution[1]

**Hisashi Mizutani,* Ikuko Miyahara,* Ken Hirotsu,*,[2] Yasuzo Nishina,† Kiyoshi Shiga,† Chiaki Setoyama,‡ and Retsu Miura‡**

*Department of Chemistry, Faculty of Science, Osaka City University, Sugimoto, Sumiyoshi-ku, Osaka 558; and Departments of †Physiology and ‡Biochemistry, Kumamoto University School of Medicine, Honjo, Kumamoto 860

Received for publication, March 27, 1996

**The X-ray crystallographic structure of porcine kidney D-amino acid oxidase, which had been expressed in *Escherichia coli* transformed with a vector containing DAO cDNA, was determined by the isomorphous replacement method for the complex form with benzoate. The known amino acid sequence, FAD and benzoate were fitted to an electron density map of 3.0 Å resolution with an *R*-factor of 21.0%. The overall dimeric structure exhibits an elongated ellipsoidal framework. The prosthetic group, FAD, was found to be in an extended conformation, the isoalloxazine ring being buried in the protein core. The ADP moiety of FAD was located in the typical $\beta\alpha\beta$ dinucleotide binding motif, with the $\alpha$-helix dipole stabilizing the pyrophosphate negative charge. The substrate analog, benzoate, is located on the *re*-face of the isoalloxazine ring, while the *si*-face is blocked by hydrophobic residues. The carboxylate group of benzoate is ion-paired with the Arg283 side chain and is within interacting distance with the hydroxy moiety of Tyr228. The phenol ring of Tyr224 is located just above the benzene ring of benzoate, implying the importance of this residue for catalysis. There is no positive charge or $\alpha$-helix dipole near N(1) of flavin. Hydrogen bonds were observed at C(2)=O, N(3)-H, C(4)=O, and N(5) of the flavin ring.**

**Key words: D-amino acid oxidase, enzyme-ligand interaction, flavoenzyme, three dimensional structure, X-ray crystallography.**

D-Amino acid oxidase [D-amino acid:$O_2$ oxidoreductase (deaminating), EC 1.4.3.3] (DAO), which catalyzes the oxidative deamination of D-amino acids, is widely distributed in living organisms, ranging from microbes to mammals. Despite the controversial roles of this enzyme in each organism, DAO has been one of the most extensively investigated flavoenzymes, since its discovery by Krebs more than 60 years ago (*1, 2*). Despite the vast accumulation of experimental results and the interpretations thereof (*3*), the catalytic mechanism of DAO remains a matter to be settled. The most influential information for mechanistic reconciliation is the three-dimensional structure at atomic resolution. We report herein the crystallographic structure of DAO in its complex form with the substrate analog, benzoate, at 3.0 Å resolution.

The expression of porcine kidney DAO by *Escherichia coli*, and the purification of the expressed enzyme and its crystallization together with preliminary crystallographic analysis have been reported elsewhere (*4*). The DAO-benzoate complex was crystallized at pH 6.3, belonging to space group, $P2_12_12_1$, with cell dimensions of $a=110.3$ Å, $b=92.9$ Å, and $c=71.6$ Å, and containing two subunits (each with 347 amino acid residues) related by a non-crystallographic two-fold axis in an asymmetric unit. Data sets for the DAO-benzoate complex and its heavy atom derivatives were collected with a Rigaku R-AXIS IIc imaging plate detector with graphite-monochromated Cu-$K\alpha$ X-rays (40 kv, 100 mA), and processed with the R-AXIS software (T. Higashi, Rigaku, Akishima).

The structure of DAO was determined for a crystal of the benzoate-bound complex by the multiple isomorphous replacement (MIR) method, using four isomorphous data sets (Table I). The scaling of all data and map calculations were performed with the CCP4 program suite of programs (*5*). The difference Patterson map calculated for the *m*-iodobenzoate derivative allowed clear interpretation of the two iodine sites. The positions of the other heavy atom sites were determined from difference Fourier maps based on iodine phasing. Refinement of the heavy atom parameters and calculation of the initial phases to 3.0 Å were performed with program MLPHARE (CCP4). The phases were greatly improved by the process of solvent flattening (*6*) and non-crystallographic symmetry averaging (*7*), using program DM (CCP4).

A partial model of one subunit consisting of 270 out of the 347 residues and FAD was built with program O (*8*). One of the other subunit was obtained by taking advantage of the non-crystallographic twofold axis. The phases calculated from this model were combined with SIGMAA (*9*) with the MIR phases. This procedure allowed us to build a model of the DAO-benzoate complex, which was complete apart

[1] This study was supported in part by Grants-in-Aid for Scientific Research [No. 07224211 (Priority Areas) and No. 07458160] from the Ministry of Education, Science, Sport and Culture of Japan.

[2] To whom correspondence should be addressed: Phone: +81-6-605-2557, Fax: +81-6-605-2522, E-mail: hirotsu@sci.osaka-cu.ac.jp

Abbreviations: DAO, D-amino acid oxidase; EMTS, ethyl mercury thiosalicylate; MIR, multiple isomorphous replacement.

TABLE I. **Data sets utilized for MIR phasing.**

| Dataset | Soak condition[a] | Maximum resolution | Unique reflections | Completeness (%) | $R_{merge}$ (%) | $R_{diff}$[b] (%) | No. of sites | Phasing power[c] |
|---|---|---|---|---|---|---|---|---|
| Native | | 3.0 | 14,054 | 94.9 | 8.25 | | | |
| EMTS | 1.0 mM, 5 d | 3.0 | 15,010 | 98.1 | 9.32 | 18.1 | 6 | 1.5 |
| $HgCl_2$ | 1.0 mM, 1 h | 4.0 | 6,552 | 98.9 | 6.15 | 9.2 | 4 | 1.2 |
| $CH_3HgCl$ | 2.0 mM, 1 h | 3.0 | 14,912 | 97.4 | 10.28 | 19.8 | 8 | 1.2 |
| *m*-$IC_6H_4COOH$ | 1.0 mM, 5 d | 3.0 | 12,086 | 81.6 | 6.01 | 12.1 | 2 | 0.7 |

[a]The soak time is given in hours (h) and days (d). [b]$R_{diff} = \Sigma||F_{PH}| - |F_P||/\Sigma|F_P|$, where $|F_{PH}|$ and $|F_P|$ are the derivative and native structure-factor amplitudes, respectively. [c]Phasing power is the ratio of the root mean square (r.m.s.) of the heavy atom scattering amplitude and the lack of closure error.

from residues 341-347. The structure was refined by simulated annealing and energy minimization with non-crystallographic restraints using program XPLOR (*10*). The entire structure was scrutinized by successively omitting 5-residue segments of the model from the phasing calculation and inspecting the resulting map. The electron density map for FAD calculated from the model is shown in Fig. 1. The final crystallographic *R*-factor was 21.0%, and the free *R*-factor was 28.7% for the data between 8.0 and 3.0 Å. The structure lacks the C-terminal seven residues for which no convincing density was obtained. The r.m.s. deviations from ideal bond lengths and bond angles are 0.011 Å and 1.8°, respectively. Analysis of the stereochemistry with PROCHECK (*11*) showed that 99.7% of the main chain atoms fall within the allowed regions of the Ramachandran plot.

Figure 2 shows the overall dimeric structure of the DAO-benzoate complex with an elongated ellipsoidal shape. The two subunits, which are related through a non-crystallographic twofold axis, do not intrude into each other extensively. Each subunit comprises two regions, though the inter-region boundary is not entirely clear. One region is characterized by an $\alpha/\beta$ structure with an open twisted $\beta$-sheet of six $\beta$-strands, which are all parallel except for the terminal one, and four $\alpha$-helices. The other region forms a pseudo $\beta$-barrel structure consisting of two twisted $\beta$-sheets, *i.e.*, one antiparallel $\beta$-sheet with five strands and another with three strands, and two parallel $\beta$-strands at the junction of the two sheets. The prosthetic group, FAD, is in an extended conformation; the adenine moiety is located in the former region, while the flavin ring resides in the latter. The active site of the enzyme is located in the cleft made up by the pseudo barrel and the boundary of the former region mentioned above. The barrel wall seems to limit the size of the substrate-binding pocket. The N-terminal region, which is a part of the open $\alpha/\beta$ structure, makes up the $\beta\alpha\beta$ motif characteristic of a dinucleotide binding site (*12*), the $\alpha$-helix, as a helix dipole, being situated so as to stabilize the negative charge of the pyrophosphate moiety (Fig. 3). The loop starting from the C-terminus of the $\beta\alpha\beta$ motif goes along the pyrophosphate and ribityl moieties, and reaches the *si*-face of the flavin ring. The consensus GXGXXG sequence is located in the $\beta$-$\alpha$ junction. The hydrophobic stretch, Val47-Ala48-Ala49-Gly50, covers the *si*-face, with respect to N(5), of the isoalloxazine nucleus, blocking the access of substrates to the *si*-face. This is consistent with the hypothesis that the catalytic event occurs on the *re*-face of flavin (*13*).

Figure 4 shows the geometrical arrangement of flavin, benzoate, and the residues constituting the active site and those in its neighborhood, together with the hydrogen-bonding network associated with flavin and benzoate. The benzoate ring lies on the *re*-face of flavin in accordance with the *re*-face specificity of DAO (*13*), as stated above. The planes of the benzoate molecule and flavin ring are parallel but not in a true face-to-face manner. This is in accord with the observation that benzoate forms a non-charge-transfer type complex with DAO (*14*). The side chain of Arg283 extends above the xylene portion of flavin. The carboxylate group of benzoate interacts with the guanidino moiety of Arg283, forming a side-on type ion-pair (*15*). This arginine residue is conserved in DAOs from different sources (*16, 17*), and our finding is consistent with the argument of Gadda *et al.* (*17*) that Arg283 may act as the carboxylate recognition site on the basis of the results of chemical modification studies with DAO from *Rhodotorula gracilis*. The hydroxyl oxygen of Tyr228 is 2.8 Å from one of the carboxylate oxygens of benzoate, suggesting strongly that Tyr228 acts as the carboxylate binding site in cooperation with Arg283. Tyr224 lies just above the plane of the benzene ring of benzoate, the two planes facing in a parallel orientation. Taking into account the orientation of Tyr224 with respect to the substrate analog, benzoate, we speculate that this residue plays a critical role in the early stage of the reductive half reaction, though it is still too early to draw a definite conclusion as to the role of Tyr224. Note that the three planes, *i.e.*, flavin, benzoate and the phenol moiety of Tyr224, are parallel, with interplanar angles ranging from 5° to 11°, whereas the ring system of Tyr228 makes an average angle of 109° with the three parallel planes. That the two tyrosine residues, Tyr224 and Tyr228, are in direct contact with the substrate analog, benzoate, is consistent with the recent observations (*18*) that mutations at these positions affect the catalytic activity of the enzyme. There is one other tyrosine residue, Tyr55, not very far away from the binding site. This residue is situated on the other side of Tyr224 facing benzoate, so direct interaction with benzoate is improbable. Tyr55 had been implied to be involved in the active site by a chemical modification study (*19*), but its involvement has been ruled out by a mutation study (*20*). Being not very far away from the active site, this residue may have an indirect effect on the catalysis. Other residues which have been postulated to be near the active site, based on either chemical modification or mutation studies, are not found at or near the active site. One such residue is His307 which is affinity labeled by D-propargylglycine accompanying the loss of activity (*21*), and the mutation of which to leucine totally abolishes the activity (*22*). However, this residue is located toward the periphery of the protein (not shown), ruling out the possibility of direct interaction of His307 with the substrate.

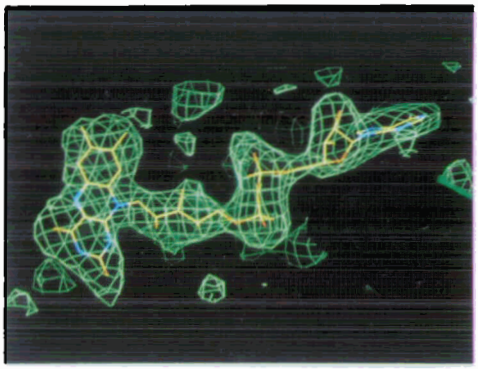

Fig. 1. **A view of the electron density for FAD.** A ($|F_o|-|F_c|$) difference map calculated from the final model and contoured at the level of $1.5\sigma$ is shown.

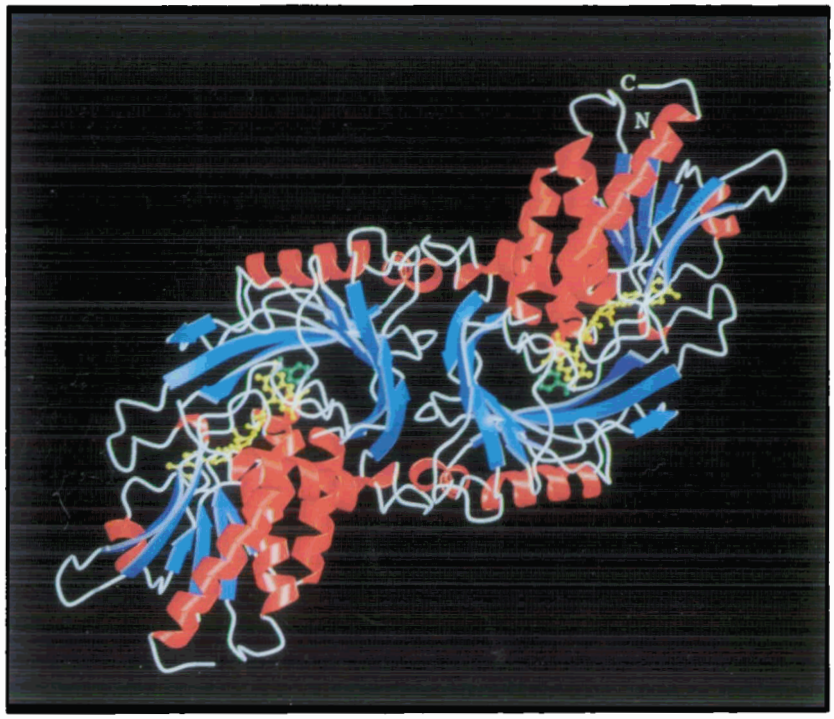


Fig. 2. **The overall dimeric structure of the DAO-benzoate complex with the non-crystallographic twofold axis running vertically, showing $\beta$-strands (blue), $\alpha$-helices (red), and loops (white).** FAD (yellow) and benzoate (green) are shown as ball and stick models. The figure was generated with programs Molscript (*26*) and Raster3D (*27*).

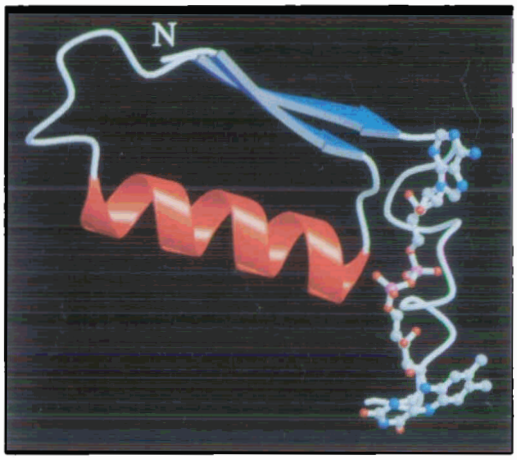


Fig. 3. **The FAD-binding site of DAO showing the typical $\beta\alpha\beta$ motif for a dinucleotide-binding site, including the long loop(Asp37–Gly50) with a short $\alpha$-helix.** The *si*-face of the flavin system is blocked by the hydrophobic stretch (see the text). The $\alpha$-helices are in red, the $\beta$-strands in blue, the loop in white, and FAD in balls and sticks.

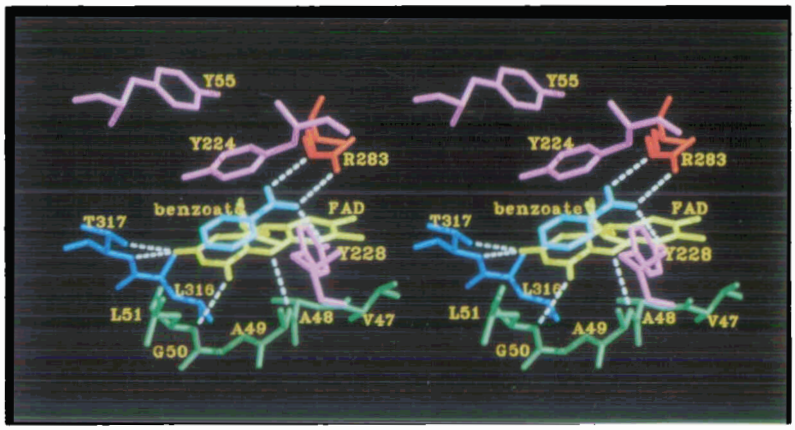


Fig. 4. **A stereoview of the active site of the DAO-benzoate complex, involving Arg283 (red), Tyr 55, 224, 228 (magenta), Val47-Leu51 (green), and Leu316-Thr317 (blue), in addition to flavin (yellow) and benzoate (cyan).** Hydrogen bonds are shown by dotted lines (white). This figure was generated with MIDAS (*28*).

One of the factors that control or influence the reactivity of flavin is the hydrogen-bonding network including the flavin nucleus (*23, 24*). The hydrogen bonds associated with the isoalloxazine framework are shown in Fig. 4. C(2)=O of flavin forms strong hydrogen bonds with the backbone N–H of Leu316 (3.05 Å) and Thr317 (2.91 Å), and with the hydroxy group of Thr317 (2.97 Å). Flavin N(3)–H is within a strongly hydrogen-bonding distance (2.90 Å) from the backbone carbonyl of Leu51. A weak hydrogen bond may be formed between C(4)=O of flavin and the backbone N–H of Leu51, as implied by the distance of 3.23 Å. Another weak hydrogen bond is suggested between N(5) of flavin and the

backbone N-H of Ala49, the distance between the nitrogen atoms being 3.21 Å. If the mutual orientation of the two nitrogens is taken into account, the hydrogen bond may be of the H-$\pi$ type rather than the normal N-H···:N type. The strong hydrogen-bonding interaction at C(2)=O and the weak one at C(4)=O in the DAO-benzoate complex are in accordance with the proposal based on a $^{13}$C-NMR study (*24*). We emphasize here that no hydrogen bond is observed at N(1). Nor is there any positive charge in the vicinity of N(1) to stabilize the negative charge generated in the reduced form of flavin. In this context, we recently postulated that the negative charge of reduced flavin at N(1) can be stabilized by the protonated positive imino nitrogen of the imino acid in the purple intermediate (*25*).

The refinement of the structure at higher resolution, and structure determination of DAO without a ligand and with ligands of other types are in progress. We are also performing structural elucidation of the intermediary states which appear during the catalysis and can be stabilized under certain conditions. The information provided in this report and that expected from the studies in progress will offer essential clues for elucidation of the reaction mechanism of DAO, which has been and still is a focus in the field of flavoenzyme catalysis in general.

## REFERENCES


1. Krebs, H.A. (1935) Metabolism of amino-acids. III. Deamination of amino acids. *Biochem. J.* **29**, 1620-1644
2. Krebs, H.A. (1951) Oxidation of D-amino acids in *The Enzymes* (Sumner, J.B. and Myrbäck, K., eds.) Vol. 2, part 1, pp. 499-535, Academic Press, New York
3. Curti, B., Ronchi, S., and Simonetta, M.P. (1992) D- and L-amino acid oxidases in *Chemistry and Biochemistry of Flavoenzymes* Vol. III, pp. 69-94, CRC Press, Boca Raton, Ann Arbor, London
4. Setoyama, C., Miura, R., Nishina, Y., Shiga, K., Mizutani, H., Miyahara, I., and Hirotsu, K. (1996) Crystallization of expressed porcine kidney D-amino acid oxidase and preliminary X-ray crystallographic characterization. *J. Biochem.* **119**, 1114-1117
5. Collaborative Computational Project, Number 4 (1994) The CCP4 suite: Programs for Protein Crystallography. *Acta Crystallogr.* **D50**, 760-763
6. Wang, B.-C. (1985) Resolution of phase ambiguity in macromolecular crystallography. *Methods Enzymol.* **115**, 90-112
7. Bricogne, G. (1974) Geometric sources of redundancy in intensity data and their use for phase determination. *Acta Crystallogr.* **A30**, 395-405
8. Jones, T.A., Zou, J.-Y., Cowan, S.W., and Kjeldgaard, M. (1991) Improved methods for building protein models in electron density maps and the location of errors in these models. *Acta Crystallogr.* **A47**, 110-119
9. Read, R.J. (1986) Improved Fourier coefficients for maps using phases from partial structures with errors. *Acta Crystallogr.* **A42**, 140-149
10. Brünger, A.T., Kuriyan, J., and Karplus, M. (1987) Crystallographic R factor refinement by molecular dynamics. *Science* **235**, 458-460
11. Laskowski, R.A., MacArthur, M.W., Moss, D.S., and Thornton, J.M. (1993) PROCHECK: A program to check the stereochemical quality of protein structures. *J. Appl. Crystallogr.* **26**, 283-291
12. Wierenga, R.K., De Maeyer, M.C.H., and Hol, W.G.J. (1985) Interaction of pyrophosphate moieties with $\alpha$-helixes in dinucleotide binding proteins. *Biochemistry* **24**, 1346-1357
13. Manstein, D.J., Ghisla, S., Massey, V., and Pai, E.F. (1988) Stereochemistry and accessibility of prosthetic groups in flavoproteins. *Biochemistry* **27**, 2300-2305
14. Massey, V. and Ganther, H. (1965) On the interpretation of the absorption spectra of flavoproteins with special reference to D-amino acid oxidase. *Biochemistry* **4**, 1161-1173
15. Mitchell, J.B.O., Thornton, J.M., Singh, J., and Price, S.L. (1992) Towards an understanding of the arginine-aspartate interaction. *J. Mol. Biol.* **226**, 251-262
16. Miyake, Y., Fukui, K., Momoi, K., Watanabe, F., Tada, M., Miyano, M., and Takahashi, S. (1991) Molecular biological studies on structure-function relationship of D-amino acid oxidase in *Flavins and Flavoproteins 1990* (Curti, B., Ronchi, S., and Zanetti, G., eds.) pp. 135-142, Walter de Gruyter, Berlin, New York
17. Gadda, G., Negri, A., and Pilone, M.S. (1994) Reaction of phenylglyoxal with arginine groups in D-amino acid oxidase from Rhodotorula gracilis. *J. Biol. Chem.* **269**, 17809-17814
18. Pollegioni, L., Fukui, K., and Massey, V. (1994) Studies on the kinetic mechanism of pig kidney D-amino acid oxidase by site-directed mutagenesis of tyrosine 224 and tyrosine 228. *J. Biol. Chem.* **269**, 31666-31673
19. Swenson, R.P., Williams, C.H., Jr., and Massey, V. (1982) Chemical modification of D-amino acid oxidase. Amino acid sequence of the tryptic peptides containing tyrosine and lysine residues modified by fluorodinitrobenzene. *J. Biol. Chem.* **257**, 1937-1944
20. Watanabe, F., Fukui, K., Momoi, K., and Miyake, Y. (1988) Effect of site-specific mutagenesis of tyrosine-55, methionine-110 and histidine-217 in porcine kidney D-amino acid oxidase on its catalytic function. *FEBS Lett.* **238**, 269-272
21. Ronchi, S., Minchiotti, L., Galliano, M., Curti, B., Swenson, R.P., Williams, C.H., Jr., and Massey, V. (1982) The primary structure of D-amino acid oxidase from pig kidney. II. Isolation and sequence of overlap peptides and the complete sequence. *J. Biol. Chem.* **257**, 8824-8834
22. Watanabe, F., Fukui, K., Momoi, K., and Miyake, Y. (1989) Site-specific mutagenesis of lysine-204, tyrosine-224, tyrosine-228, and histidine-307 of porcine kidney D-amino acid oxidase and the implications as to its catalytic function. *J. Biochem.* **105**, 1024-1029
23. Nishimoto, K., Fukunaga, H., and Yagi, K. (1986) Studies in a model system on the effect of hydrogen bonding at hetero atoms of oxidized flavin on its electron acceptability. *J. Biochem.* **100**, 1647-1653
24. Miura, R. and Miyake, Y. (1987) $^{13}$C-NMR studies on the reaction intermediates of porcine kidney D-amino acid oxidase reconstituted with $^{13}$C-enriched flavin adenine dinucleotide. *J. Biochem.* **102**, 1345-1354
25. Nishina, Y., Sato, K., Miura, R., and Shiga, K. (1995) Structure of charge-transfer complexes of flavoenzyme D-amino acid oxidase: A study by resonance Raman spectroscopy and extended Hückel molecular orbital method. *J. Biochem.* **118**, 614-620
26. Kraulis, P.J. (1991) Molscript: A program to produce both detailed and schematic plots of protein structures. *J. Appl. Crystallogr.* **24**, 946-950
27. Merritt, E.A. and Murphy, M.E.P. (1994) Raster3D version 2.0. A program for photorealistic molecular graphics. *Acta Crystallogr.* **D50**, 869-873
28. Ferrin, T.E., Huang, C.C., Jarvis, L.E., and Langridge, R. (1988) The MIDAS display system. *J. Mol. Graphics* **6**, 13-27